A mitochondrial-targeted cyclosporin A with high binding affinity for cyclophilin D yields improved cytoprotection of cardiomyocytes

Henry DUBE*, David SELWOOD*, Sylvanie MALOUITRE†, Michela CAPANO†, Michela I. SIMONE*[1] and Martin CROMPTON†[2]

*Wolfson Institute for Biomedical Research, University College London, Gower Street, London WC1E 6BT, U.K., and †Institute of Structural and Molecular Biology, University College London, Gower Street, London WC1E 6BT, U.K.

Mitochondrial CyP-D (cyclophilin-D) catalyses formation of the PT (permeability transition) pore, a key lesion in the pathogenesis of I/R (ischaemia/reperfusion) injury. There is evidence [Malouitre, Dube, Selwood and Crompton (2010) Biochem. J. **425**, 137–148] that cytoprotection by the CyP inhibitor CsA (cyclosporin A) is improved by selective targeting to mitochondria. To investigate this further, we have developed an improved mtCsA (mitochondrial-targeted CsA) by modifying the spacer linking the CsA to the TPP$^+$ (triphenylphosphonium) (mitochondrial-targeting) cation. The new mtCsA exhibits an 18-fold increase in binding affinity for CyP-D over the prototype and a 12-fold increase in potency of inhibition of the PT in isolated mitochondria, owing to a marked decrease in non-specific binding. The cytoprotective capacity was assessed in isolated rat cardiomyocytes subjected to transient glucose and oxygen deprivation (pseudo-I/R). The new mtCsA was maximally effective at lower concentrations than CsA (3–15 nM compared with 50–100 nM) and yielded improved cytoprotection for up to 3 h following the pseudo-ischaemic insult (near complete compared with 40 %). These data indicate the potential value of selective CyP-D inhibition in cytoprotection.

Key words: cyclophilin D (CyP-D), cyclosporin, ischaemia, mitochondrial targeting, reperfusion injury (RI), triphenylphosphonium (TPP$^+$).

INTRODUCTION

Myocardial ischaemia is a major cause of death and disability. Minimizing tissue injury requires early restoration of blood flow. After prolonged ischaemia, however, still surviving cells become adversely affected by restored blood supply and succumb on reperfusion. RI (reperfusion injury) is a complicating factor in clinical procedures used to remove a coronary obstruction (angioplasty, thrombolysis and bypass surgery) and in organ transplantation.

Considerable evidence implicates the PT (permeability transition) pore model of necrotic cell death [1,2] in RI. The non-selective PT pore forms in the mitochondrial inner membrane under the synergistic influence of high Ca^{2+} concentration [3], oxidative stress [1] and depleted adenine nucleotides [2], factors common to RI. The resulting collapse of the proton electro-chemical gradient allows the ATP synthase to operate in reverse, catalysing rapid ATP hydrolysis [1] and leading to irreversible cell injury. The molecular identity of the PT pore is controversial. Reconstitution studies indicate that the pore forms from a malfunctioning adenine nucleotide translocase [4–6], but additional, or alternative, transport proteins, e.g. the phosphate carrier [7], have also been considered. It is generally agreed, however, that PT pore formation is catalysed or stabilized by CyP (cyclophilin)-D, an intra-mitochondrial peptidylprolyl cis–trans-isomerase. CyP-D is regulated by acetylation, which potentiates its binding to the adenine nucleotide translocase and lowers the Ca^{2+} threshold for PT pore formation [8]. The CyP inhibitor CsA (cyclosporin A) blocks pore formation and gives partial protection in isolated cardiomyocyte [9], perfused heart [10] and mouse [11] models of RI. PT pore opening is promoted by CyP-D overexpression [12] and is attenuated by CyP-D knockout [13]. Genetic ablation of CyP-D reduces infarct size in heart [14] and other tissues (brain [15] and kidney [16]), and is also protective in models of degenerative diseases, i.e. Alzheimer's disease [17], multiple sclerosis [18], muscular dystrophy [19] and motor neuron disease [20].

Thus the PT pore appears to be an intrinsic feature of RI and many other diseases leading to lethal cell injury, and, in controlling PT pore formation, CyP-D offers a potential target for pharmacological intervention. However, CsA may exert variable effects on cell viability owing to its interaction with cytosolic CyP-A and other non-mitochondrial CyPs. Recently, we have shown that targeting CsA to mitochondria, thereby minimizing extra-mitochondrial interactions, improves cytoprotection in an isolated neuronal model of 'energy failure' [21]. In the present paper, we report the synthesis of a modified mtCsA (mitochondrial-targeted CsA) with a much-improved CyP-D-binding affinity over the prototype, and show that it yields better cytoprotection than CsA in an isolated cardiomyocyte model of RI.

EXPERIMENTAL

Synthesis of cyclosporin analogues

A scheme of the syntheses is given in Figure 1. Compound **2**, SMBz-CsA {[sarcosine-3(4-methylbenzoate)]-CsA}, was used as a key intermediate in the synthesis of the alkyl-linked TPP$^+$ (triphenylphosphonium) analogue (compound **5**), as described previously [21] and in the new alkyl linked rosamine (compound **6**) and ether-linked TPP$^+$ (compound **9**) analogues as
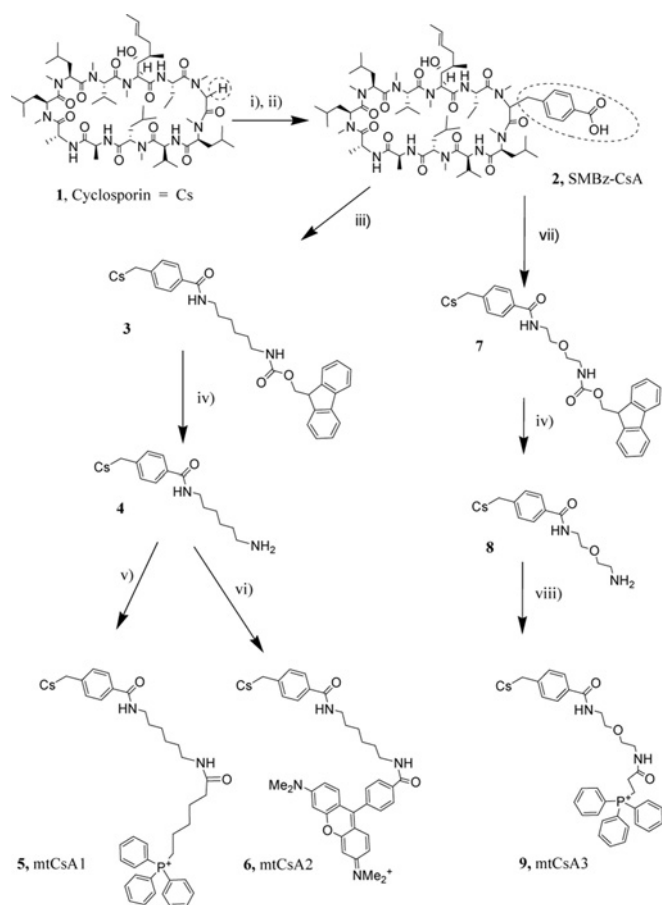
Figure 1   Chemical synthesis of the CsA analogues

The dotted circles show the position of alkylation at the (Sar-3) of cyclosporin **1** and the appended methylbenzoic acid group in SMBz–CsA **2**. For simplicity cyclosporin in the structures **3**–**9** is drawn as Cs. The reagents used in each step are: (i) lithium di-isopropylamide, THF; 4-(BrCH₂)PhCOOMe; (ii) LiOH, methanol; (iii) 1-Fmoc-1,6-diaminohexane, PyBOP, triethylamine (Et₃N), THF; (iv) piperidine, DMF; (v) 5-(carboxypentyl)triphenylphosphonium bromide, PyBOP, Et₃N, THF; (vi) Rosamine acid, PyBOP, Et₃N, THF; and (vii) 2-[2-(Fmoc-amino)ethoxylamine]. HCl, PyBOP, Et₃N, THF; and (viii) 2-(carboxyethyl)triphenylphosphonium bromide.

described below. LC (liquid chromatography)–MS was run on an Agilent 6130 system, using a C_4 reverse-phase column with the standard programme. Solvent A was 95 % water, 5 % methanol and 0.1 % formic acid. Solvent B was 5 % water, 95 % methanol and 0.1 % formic acid. Elution was with a 50 % solvent A gradient to 95 % solvent B over 7 min then 95 % solvent B for 8 min.

Compound 6, mtCsA2

To a solution of the amine **4** [21] (57 mg, 0.0397 mmol) in THF (tetrahydrofuran; 2.5 ml) was added rosamine acid [22] (46 mg, 0.119 mmol), PyBOP (benzotriazol-1-yl-tris-pyrrolidinophosphonium hexafluorophosphate; 41 mg, 0.18 mmol) and triethylamine (20 mg, 0.19 mmol) under argon at room temperature (22 °C). The reaction mixture was stirred for 24 h at room temperature. The volatiles were removed *in vacuo* to leave a yellow oil. The oil was purified by flash column chromatography on silica gel eluting with 6 % methanol in DCM (dichloromethane) followed by methanol/DCM/NH₃ (aq) (1:8:1, by vol.) to give the title compound (10.1 mg, 0.0056 mmol, 14 %) as a red solid. ESI (electrospray ionization)– TOF (time-of-flight) MS in positive-ion mode: calculated m/z for $C_{100}H_{153}N_{15}O_{15}+$,

1804.1671; found m/z 1804.0834; mDa − 83.7; p.p.m. − 46.4; LC–MS broad peak eluting at 7 min.

Compound 7, Fmoc (fluoren-9-ylmethoxycarbonyl)-protected amine

To a stirred solution of the acid 2, SMBz-CsA (100 mg, 0.07 mmol) in dry THF (6.0 ml) was added 2-[2-(Fmoc-amino)ethoxylamine] hydrochloride (70.0 mg, 0.12 mmol), HATU [2-(7-aza-1*H*-benzotriazole-1-yl-1)-1,3,3-tetramethyl-uronium hexafluorophosphate] (70.0 mg, 0.12 mmol) and triethylamine (0.36 mmol, 0.1 ml) under nitrogen at room temperature and the resultant mixture was stirred for 24 h. Then DCM (15 ml) followed by saturated NH₄Cl (aq) (5 ml) were added. The mixture was extracted with DCM (2×3 ml), and dried using anhydrous MgSO₄. The volatiles were removed *in vacuo* to leave a brown oil residue. Purification by chromatography (SiO₂, 5 % methanol/DCM) gave the Fmoc-protected derivative **7** (100 mg, 0.61 mmol, 82 %): as a white solid. ESI–TOF MS in positive-ion mode: calculated m/z for $C_{89}H_{137}N_{13}O_{16}Na+$, 1668.0282; found m/z 1668.0624; mDa − 34.2; p.p.m. 20.5.

Compound 8, amine

A solution of the Fmoc compound **7** (90 mg): was stirred in 20 % piperidine in DMF (dimethylformamide; 4 ml) under argon for 24 h. The volatiles were removed *in vacuo* to leave a yellow oil. The oil was purified by flash column chromatography on silica gel eluting with 6 % methanol in DCM followed by methanol/DCM/NH₃ (aq) (1:8:1, by vol.) to afford the amine **8** (55 mg, 0.04 mmol, 80 %) as a yellow solid and was used directly for the next step. LC–ESI MS in positive-ion mode $C_{74}H_{127}N_{13}O_{14}$ m/z 1424.47 ($M+1$), 712.24 ($M+2$).

Compound 9, mtCsA3

To a solution of the amine **8** (50 mg, 0.035 mmol) in THF (1 ml) was added (2-carboxyethyl)triphenylphosphonium bromide (30 mg, 0.07 mmol), HATU (30 mg, 0.07 mmol) and triethylamine (0.70 mmol, 0.1 ml) under argon at room temperature. The reaction mixture was stirred for 24 h at room temperature. The volatiles were removed *in vacuo* to leave a yellow oil. The oil was purified by flash column chromatography on silica gel eluting with 6 % methanol in DCM followed by methanol/DCM/NH₃ (aq) (1:8:1, by vol.) to afford mtCsA3 (40 mg, 0.029 mmol, 82 %) as a white solid. ESI MS in positive-ion mode: calculated m/z for $C_{95}H_{145}N_{13}O_{15}P+$ 1740.0799; found m/z 1740.0155.

Interactions of CsA analogues with CyPs and calcineurin

Recombinant rat CyP-D and CyP-A were prepared and purified as described previously [12,21]. CyP binding of CsA analogues was measured from the inhibition of PPIase (peptidylprolyl *cis–trans*-isomerase) activity and is expressed as an inhibitor (dissociation) constant K_i. PPIase assays were conducted at 15 °C in 100 mM NaCl/20 mM Hepes (pH 7.5) using the chromophoric test peptide *N*-succinyl-alanyl-alanyl-prolyl-4-nitroanilide [12]. K_i values were determined using the Henderson equation for a tight binding competitive inhibitor as described previously [21]. Linear plots were each derived from >6 rate measurements over >10-fold range of inhibitor concentrations and best fitted by linear regression (as in Figure 2A of [21]). Interaction of the CyP–CsA analogue complexes with calcineurin was determined from the inhibition of the phosphatase activity of calcineurin as assayed by the release of P_i from the RII phosphopeptide (Biomol International).
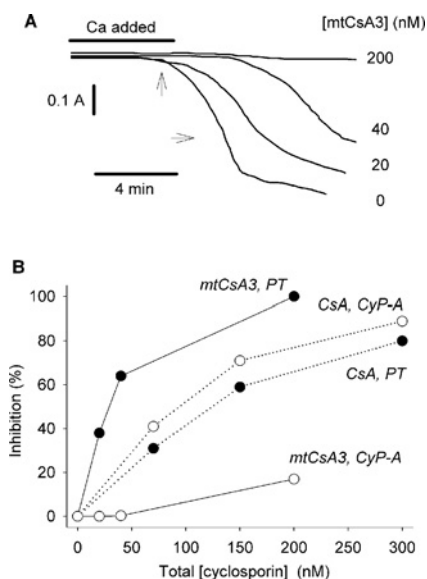
Figure 2   Preferential inhibition of intra-mitochondrial CyP-D rather than extra-mitochondrial CyP-A by mtCsA3

(**A**) Isolated mitochondria were incubated with added recombinant CyP-A and the indicated concentrations of mtCsA3. CyP-D-dependent PT pore opening was induced by Ca^{2+} and monitored from the decrease in A_{540} due to mitochondrial swelling. (**B**) Continuous lines, the rate of PT pore opening in (**A**) was determined from the time taken [from the vertical arrow in (**A**)] to decrease absorbance by 0.24 unit [horizontal arrow in (**A**)] and plotted as inhibition by mtCsA3 (mtCsA3, PT). In a parallel incubation, mitochondria were sedimented immediately after addition of $CaCl_2$ and the inhibition of CyP-A by mtCsA3 was determined (mtCsA3, CyP-A). Broken lines inhibition of the PT and CyP-A by CsA was measured as described above for mtCsA3. Data for mtCsA3 and CsA are representative of three experiments.

PT pore opening in isolated mitochondria

Isolated rat liver mitochondria [12] (3 mg of protein) were incubated with continuous stirring in 3 ml of 120 mM KCl/2 mM KH_2PO_4/3 mM succinate/1 μM rotenone/5 μM EGTA/recombinant CyP-A and test cyclosporins as indicated. After 5 min, $CaCl_2$ was added at a constant rate of 10 μM/min to a final concentration of 50 μM. PT pore opening was monitored from mitochondrial swelling according to the decrease in absorbance at 540 nm [21]. In an identical parallel incubation mitochondria were sedimented immediately after $CaCl_2$ addition and the CyP-A activity in the supernatant was determined.

Cardiomyocyte culture and assays

Primary cultures of cardiomyocytes were prepared from 14-day-old Sprague–Dawley rats, seeded on to glass coverslips, and maintained under CO_2/air (1:19) as described previously [23]. All animal experiments conformed to UK Home Office legislation. For glucose-free anoxia, cells were washed twice with PBS and incubated at 25 °C under oxygen-free nitrogen in 120 mM $NaCl$/4 mM KCl/24 mM Hepes (Na^+ salt, pH 7.4)/1 mM $MgSO_4$/1 mM $CaCl_2$/1 mM KH_2PO_4/4 μM ethidium homodimer/2 μM Hoechst 33342 and cyclosporins as indicated in a 5-well system mounted on the microscope stage. After 4 h, 10 mM glucose, 5 % (v/v) foetal bovine serum and 50 μM t-butyl hydroperoxide were added, and the cells were reoxygenated by gassing with air. Fluorescence images were acquired [21] after nuclear staining with Hoechst 33342 and ethidium homodimer used to quantify total and necrotic cells respectively. Statistical analyses were made using paired Student's *t* tests and are presented as means $\pm$ S.E.M.

RESULTS AND DISCUSSION

A mitochondrial-targeted cyclosporin with improved CyP-D binding affinity

CsA (compound **1**, Figure 1) is a lipophilic cyclic undecapeptide that inhibits the PPIase activity of CyPs. CsA inhibition of the mitochondrial isoform CyP-D prevents PT pore formation and partially protects against RI in experimental models (as described in the Introduction). Recently, we reported that neuroprotection by CsA is limited by counter-protective interactions with extra-mitochondrial CyPs and that cytoprotection is improved when CyP-D is inhibited selectively [21]. CyP-D selectivity was achieved with a mitochondrial-targeted CsA, here designated mtCsA1 (compound **5**, Figure 1) in which residue 3 of the CsA ring was conjugated via a linker to the lipophilic TPP^+ cation. The positively charged mtCsA1 was accumulated electrophoretically by mitochondria in response to the negative-inside inner membrane potential, enabling selective inhibition of mitochondrial CyP-D in cells. However, the high binding affinity of CyP-D for CsA was decreased substantially by the modifications in mtCsA1, and more mtCsA1 was required for PT pore blockade than CsA itself. The first aim of the present study was therefore to investigate whether the intrinsically high binding affinity of CyP-D for CsA could be retained within this basic strategy (CsA–linker–TPP^+) of targeting CsA to mitochondria.

The synthesis of the required analogues (Figure 1) was accomplished by adaptation of our previously described method for synthesis of mtCsA1 [21]. SMBz-CsA (compound **2**) was coupled in solution to Fmoc-monoprotected diamine using the standard peptide coupling reagent PyBOP to afford the corresponding Fmoc-protected amide intermediate **3**. This intermediate was deprotected by reaction with piperidine in DMF to give amine **4** and coupled in solution to rosamine acid [22] with PyBOP and triethylamine to produce target compound **6**. The ether-linked compounds **7**–**9** were prepared using similar methods.

CyP-binding affinities for CsA analogues were determined from PPIase inhibition, and are reported as inhibitor (dissociation) constants in Table 1. CyP-D bound the prototype mtCsA compound, mtCsA1, with an affinity ($K_i = 93$ nM) approximately 1/30 of that for CsA ($K_i = 3$ nM). Some loss of binding affinity in mtCsA1 might be anticipated. The CsA ring half inserts into the CyP active site with residues 9–11 and 1–3 interacting with the CyP and residues 4–8 remaining exposed to the solvent [24]. Hence position 3 additions, as in mtCsA1, might sterically hinder binding to CyP-D. Yet the additions at position-3 that form the linker caused relatively modest decreases in binding affinity (K_i values: compound **2**, 7 nM; compound **4**, 15 nM). The major loss of affinity occurred with Fmoc (K_i value for compound **3**, 160 nM) and TPP^+ (K_i value for mtCsA1, 93 nM). Addition of rosamine to the linker, as an alternative (mitochondrial-targeting) lipophilic cation to TPP^+, also decreased binding affinity considerably (K_i value for compound **6**, mtCsA2, 202 nM). These findings indicate that the large loss of binding affinity is not due specifically to TPP^+, since addition of other bulky groups caused losses at least as great, or to modification at position 3. Rather, it seems that these bulky groups are not effectively separated from the CsA by the linker, possibly as a result of hydrophobic collapse in which the linker–TPP^+ ($-$Fmoc, $-$rosamine) folds back on itself to maximize hydrophobic interactions, thereby stabilizing the TPP^+ (Fmoc, rosamine) in close proximity to the CsA. We therefore investigated the use of a shortened linker containing an ether linkage to reduce hydrophobicity.

The ether-linked derivatives are shown as compounds **7**–**9** (Figure 1). Remarkably, CyP-D bound the new Fmoc and TPP^+ derivatives with an affinity close to that for CsA (K_i values:

Table 1   Inhibition by CsA derivatives of CyPs, calcineurin and the PT pore

CsA derivatives are numbered as in Figure 1. K_i values are the inhibitor (dissociation) constants for inhibition of purified CyP-D and CyP-A; values in parentheses are the linear correlation coefficients for the lines used to derive the K_i values. Inhibition of the phosphatase activity of calcineurin was determined with 720 nM complexes of CyP-A and CsA derivatives (see text); values are the average of two measurements differing by <6%. I_{50} is defined as the total cyclosporin concentration (pmol/mg of mitochondrial protein) yielding 50% inhibition of PT pore opening in isolated mitochondria incubated as in Figure 2. Data for I_{50} and CyP-A inhibition are means ± S.E.M. (three mitochondrial preparations).
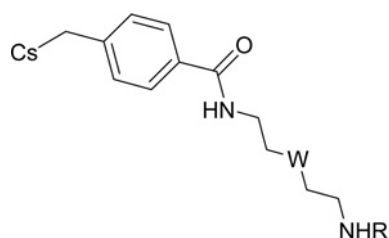
Compound	W	R	K_i (nM)		Calcineurin inhibition (%)	I_{50} for PT (pmol/mg of protein)	CyP-A inhibition at I_{50} (%)
			CyP-D	CyP-A			
1, CsA	–	–	3 (0.992)	4 (0.987)	74	125 ± 10	60 ± 7
2, SMBz- CsA	–	–	7 (0.934)	8 (0.958)	− 3	286 ± 16	–
3	(CH$_2$)$_2$	Fmoc	160 (0.955)	–	–	–	–
4	(CH$_2$)$_2$	H	15 (0.951)	–	–	–	–
5, mtCsA1	(CH$_2$)$_2$	CO(CH$_2$)$_5$PPh$_3$$^+$	93 (0.993)	115 (0.975)	− 5	353 ± 27	9 ± 1
6, mtCsA2	(CH$_2$)$_2$	Rosamine	202 (0.990)	213 (0.995)	–	770 ± 32	21 ± 6
7	0	Fmoc	6 (0.959)	–	–	–	–
9, mtCsA3	0	CO(CH$_2$)$_2$PPh$_3$$^+$	5 (0.971)	8 (0.982)	4	29 ± 3	1 ± 1

compound **7**, 6 nM; compound **9**, 5 nM). Although addition of alkyl linker and TPP$^+$ to compound **2** caused a 13-fold decrease in CyP-D-binding affinity, the addition of ether linker and TPP$^+$ caused no loss. The new mtCsA (compound **9**) is designated mtCsA3.

CsA binding to the cytosolic isoform CyP-A can also influence cell viability (described below) and, although mtCsA compounds are designed to minimize interactions with CyP-A by means of accumulation out of the cytosol into mitochondria, CyP-A data were also obtained (Table 1). CyP-A bound CsA and the mtCsA derivatives with a similar affinity as CyP-D, conforming to the close similarity between the CsA-binding sites in the two isoforms [24,25]. In addition, the CyP-A–CsA complex inhibits the protein phosphatase calcineurin [26]. To compare calcineurin inhibition by CyP-A–mtCsA complexes, the concentrations of CsA and derivatives were chosen to give the same concentration (720 nM) of their respective complexes with CyP-A (calculated from K_i values), and we confirmed that, when added alone, these concentrations of CyP-A, CsA and derivatives did not inhibit calcineurin ([21], results not shown). Table 1 shows that, although the CyP-A–CsA complex inhibits calcineurin phosphatase activity, the CyP-A complexes with the mtCsA compounds did not. The additions at position 3 of CsA in the derivatives presumably prevent binding of the CyP–CsA (derivative) complexes by calcineurin which is known to involve contacts between calcineurin and positions 3–7 of the CsA ring [24,26].

Mitochondrial accumulation of mtCsA compounds

The capacity of mitochondria to accumulate mtCsA derivatives was evaluated by comparing inhibition of the CyP-D-dependent PT pore and inhibition of extra-mitochondrial CyP-A in a system comprising isolated mitochondria and added recombinant CyP-A. PT pore opening was triggered by addition of Ca^{2+} and monitored from the resultant mitochondrial swelling (Figure 2A) [21]. Ca^{2+} uptake is electrophoretic and, when rapid, depresses $\Delta\varphi_m$ (inner membrane potential) [12]. As dissipation of $\Delta\varphi_m$ would

compromise electrophoretic accumulation of mtCsA compounds, Ca^{2+} was infused slowly over several minutes to limit the rate of Ca^{2+} influx and to prevent loss of $\Delta\varphi_m$ arising from rapid Ca^{2+} flux [21]. Extramitochondrial CyP-A activities were determined in parallel (identical) incubations (see the Experimental section).

Representative time courses of PT pore opening, showing mtCsA3 inhibition, are given in Figure 2(A); equivalent time courses were obtained for all CsA compounds analysed (I_{50} values, Table 1). To compare inhibition by the different compounds, rates were calculated from the time period between first detection of PT pore opening in the absence of inhibitor (vertical arrow, Figure 2A) and the attainment of a 0.24 unit change in absorbance (horizontal arrow; corresponding to an approximate half-maximal absorbance change). Approximately 29 nM total mtCsA3 produced 50% inhibition of PT pore opening, but no detectable inhibition of CyP-A (Figure 2B). A total mtCsA3 concentration of 200 nM yielded just 17% inhibition of CyP-A, indicating an extra-mitochondrial free mtCsA3 concentration of approximately 1.6 nM (calculated from $K_i = 8$ nM, Table 1), i.e. that nearly all mtCsA3 had been accumulated by mitochondria, with negligible amounts remaining outside for inhibition of CyP-A.

In agreement with previous data [21], CsA itself displayed no selectivity for the PT pore over extra-mitochondrial CyP-A (Figure 2B); this would be expected as CsA is bound by CyP-D and CyP-A with similar affinities (Table 1) and, being electroneutral, would equilibrate to the same free concentrations on either side of the mitochondrial inner membrane. To compare selectivities by mtCsA compounds, Table 1 (rightmost column) gives the CyP-A inhibition at 50% inhibition of the PT. mtCsA-selectivity for the PT increased with increased binding affinity for the target CyP-D (mtCsA3>mtCsA1>mtCsA2)

Non-specific binding of mtCsA compounds in mitochondria

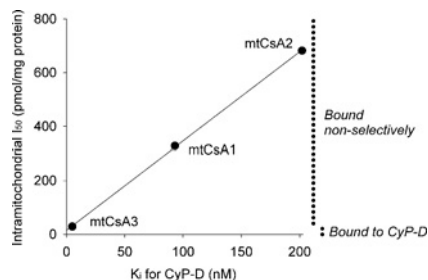In line with mitochondrial accumulation, considerably less mtCsA3 than CsA was needed for PT pore inhibition (I_{50},

Figure 3   Relationship between the potencies of mtCsA compounds as inhibitors of CyP-D and the PT

Intra-mitochondrial I_{50} values (intra-mitochondrial mtCsA concentration) yielding 50% inhibition of the PT were obtained by correcting the mean I_{50} values (Table 1) for extra-mitochondrial mtCsA concentration. The latter was estimated at each I_{50} value from the amount of extra-mitochondrial CyP-A and the degree of CyP-A inhibition: from Table 1 (and since membrane-partitioned CsA at the I_{50} is small; see text) 60% CyP-A inhibition corresponds to 96 pmol of extra-mitochondrial CsA/mg protein (I_{50} for CsA − I_{50} for mtCsA3), which indicates 150 pmol of CyP-A/mg of protein (using $K_i = 4$ nM); hence, using respective K_i values, 9% CyP-A inhibition corresponds to 25 pmol of extra-mitochondrial mtCsA1/mg of protein, and 21% CyP-A inhibition to 88 pmol of extra-mitochondrial mtCsA2/mg protein, yielding intra-mitochondrial I_{50} values of 328 (mtCsA1) and 682 (mtCsA2) pmol/mg. These values were not changed significantly when calculated from replicate I_{50} values and corresponding CyP-A-inhibition values for mtCsA1 and mtCsA2, i.e. intra-mitochondrial I_{50}: 329 ± 25 (mtCsA1) and 677 ± 6 (mtCsA2) (means $\pm$ S.E.M., $n = 3$).

29 pmol/mg compared with 125 pmol/mg; Table 1). However, in the same experimental system, more mtCsA1 was required (I_{50}, 353 pmol/mg), despite its being accumulated by mitochondria [21]. This suggests that the bulk of mitochondrially accumulated mtCsA1 was bound non-specifically. This was also the case with the other alkyl-linked derivative, mtCsA2 (I_{50}, 770 pmol/mg). In this connection, Scatchard analyses reveal that a small amount of mitochondrial CsA is partitioned into membrane phospholipids (approximately 15% at the I_{50} [27]). The amount of membrane-partitioned mtCsA would be expected to increase in direct proportion to the free mtCsA concentration in the mitochondrial matrix. In turn, the matrix free mtCsA concentration at the I_{50} will increase in proportion to the K_i value of CyP-D for that mtCsA. This would lead to a linear relationship between the amount of mitochondrial mtCsA yielding 50% PT inhibition (intra-mitochondrial I_{50}) and the free mtCsA concentration giving 50% CyP-D inhibition (K_i for CyP-D). Intra-mitochondrial I_{50} values were obtained by correcting the I_{50} values (which refer to total mtCsA) for the relatively small amounts of extra-mitochondrial mtCsA (legend, Figure 3), and these yielded the predicted linear relationship with K_i (Figure 3). Clearly, differences in lipid solubility between the mtCsA compounds would produce deviations from linearity, but any such deviations appear to be small. It is probable, therefore, that non-selective membrane binding of the mtCsA compounds was determined largely by the SMBz-CsA moiety common to all, with the remaining parts of the linkers exerting relatively little influence. Cationic mitochondrial-targeting groups, e.g. TPP$^+$, conjugated to lipophilic molecules appear to lie on the inner surface of the inner membrane with the lipophilic moiety in the membrane interior [28].

The ordinate intercept in Figure 3 (at theoretical infinite CyP-D affinity for mtCsA, when all added mtCsA is bound to CyP-D) corresponds to the amount of mtCsA bound to CyP-D at the intra-mitochondrial I_{50}. From this it is clear that, although the fraction of mitochondrially accumulated mtCsA1 and mtCsA2 actually bound to CyP-D was relatively small (3 and 1.5% respectively at the I_{50}) a far greater proportion of mtCsA3 (>50%) was CyP-D-bound.
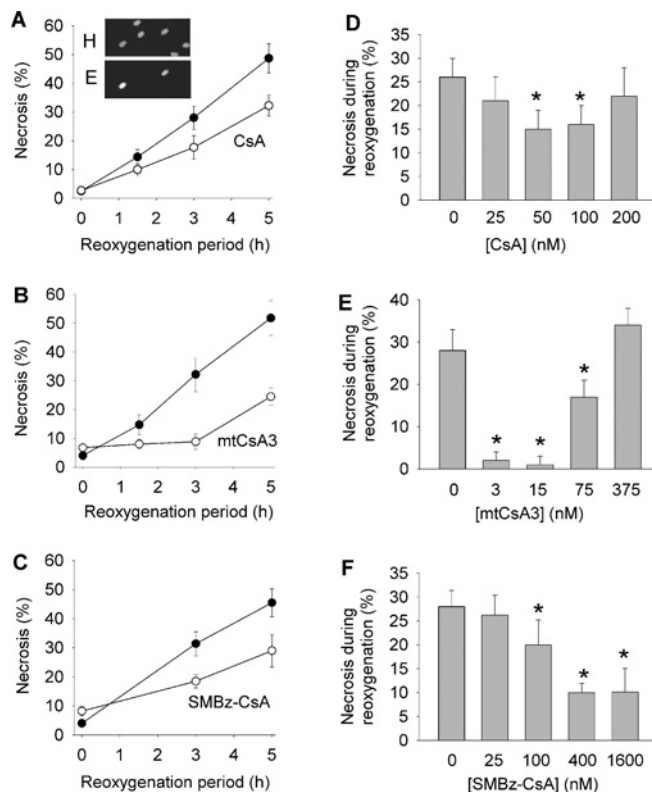

Figure 4   Inhibition of reoxygenation-induced necrosis in cardiomyocytes by CsA and derivatives

Isolated cardiomyocytes were incubated under glucose-free anoxia for 4 h and then aerobically with glucose and 50 μM t-butyl hydroperoxide (reoxygenation). When included, CsA and derivatives were added at the beginning of anoxia. (**A–C**) Cell necrosis during reoxygenation in the presence and absence of 50 nM CsA, 15 nM mtCsA3 and 400 nM SMBz–CsA, as indicated, was determined from nuclear staining with ethidium homodimer. Insets in (**A**) show cells dual-stained with Hoechst 33342 (H) and ethidium homodimer (E) after 3 h of reoxygenation. (**D** and **E**) Necrosis after 3 h of reoxygenation with the indicated concentrations of CsA, mtCsA3 and SMBz–CsA. Results are means $\pm$ S.E.M. for four cell preparations, >200 cells counted per preparation. *$P < 0.05$ with respect to no addition.

Protection by mtCsA3 in cardiomyocytes

The cytoprotective properties of the improved mtCsA compound were evaluated in isolated heart cells subjected to simulated I/R (ischaemia/reperfusion). The cells were first exposed to glucose-free anoxia to mimic ischaemia; in practice, cells could be maintained under these conditions for approximately 4 h with little necrosis (<8%). The myocytes were then reoxygenated in the presence of glucose and 50 μM t-butyl hydroperoxide, and this produced progressive cell necrosis amounting to approximately 50% after 5 h (Figures 4A–4C). t-Butyl hydroperoxide was included to boost oxidative stress, a critical component of RI [29] and of PT pore opening in cardiomyocytes [1,30]. Other experiments (results not shown) confirmed that necrosis was substantially reduced on omission of either t-butyl hydroperoxide (<15% necrosis after 5 h) or the period of glucose-free anoxia (no increase in necrosis during 5 h of reoxygenation).

After 3 h of reoxygenation, CsA gave a maximal cytoprotection of approximately 38% at 50–100 nM (Figure 4D). Increased CsA concentration to 200 nM decreased cytoprotection and, in a separate series of paired experiments, 1 μM CsA gave no protection at all (controls, 25 ± 4% necrosis; CsA tests, 25 ± 5%; $n = 4$, $P = 0.86$). This agrees with the reversal of cytoprotection with increased CsA concentration observed

previously in isolated adult rat cardiomyocytes [9], isolated rat hippocampal neurons [21] and perfused rat heart [10]. In comparison, mtCsA3 delayed the onset of necrosis completely at 3–15 nM (Figure 4E). However, protection was reversed at higher concentrations and when reoxygenation was prolonged beyond 3 h (Figure 4B).

The increased maximal cytoprotection gained by mitochondrial targeting most logically reflects avoidance of counter-protective actions of CsA external to mitochondria. These might include calcineurin inhibition by the CyP–CsA complex and/or inhibition (PPIase) of CyP-A (cytosol) or other extra-mitochondrial CyPs. To evaluate the contribution of these factors to the enhanced protection by mtCsA3, we used SMBz–CsA (compound **2**, Figure 1). Like mtCsA3, SMBz–CsA has similar binding affinities for CyP-D and CyP-A and, in complex with CyP-A, does not inhibit calcineurin (Table 1). Unlike mtCsA3, however, SMBz–CsA lacks the mitochondrial-targeting TPP$^+$ cation and is not accumulated by mitochondria, and, being freely permeable across the mitochondrial inner membrane, inhibits both CyP-D and CyP-A in cells [21]. Thus the cellular inhibition profile of SMBz–CsA (inhibiting CyP-D and CyP-A) is distinct from that of CsA (inhibiting CyP-D, CyP-A and calcineurin) and mtCsA (inhibiting CyP-D) [21]. As shown in Figure 4(D), maximal cytoprotection by SMBz–CsA (65%) was greater than that given by CsA (38%), indicating that avoidance of calcineurin inhibition may contribute to the increased potency of mtCsA3 with respect to CsA, as shown previously for mtCsA1 in neuronal cells following glucose-free anoxia [21]. However, maximal protection by the SMBz–CsA was less than that given by mtCsA3, suggesting that avoidance of inhibition of CyP-A or other extra-mitochondrial CyPs also contributes to the enhanced cytoprotection gained by mitochondrial targeting. In this connection, both CyP-A and CyP-B (sarcoplasmic reticulum) counteract oxidative stress [23,31] and inhibition of these PPIases may be counter-protective when oxidative stress is a critical element in the pathogenesis, as in the present regime.

In conclusion, we have developed a mitochondrial-targeted CsA with a binding affinity for CyP-D close to that of CsA itself. These two features, intra-mitochondrial selectivity for CyP-D and mitochondrial targeting, are designed to minimize non-CyP-D interactions in cells. In a model system, the mtCsA counters RI more effectively than CsA, underlining the potential improvement in cytoprotection to be gained by selective CyP-D inhibition. MtCsA3 is effective over a discrete concentration range (Figure 4E) and, to be useful therapeutically, will need to establish intra-mitochondrial concentrations within the effective range before PT pore formation takes place. Indications are that the pore forms quickly on reperfusion. Measurements in isolated cardiomyocytes of mitochondrial inner membrane potential [2] and Ca^{2+} accumulation capacity [32] reveal that both are lost within 1–2 min after reoxygenation in non-recovering cells, consistent with PT pore formation within this time. Since anti-RI therapeutics can only be delivered to organs on reperfusion, a key question to be resolved is whether mtCsA compounds can establish intra-mitochondrial concentrations within the effective range sufficiently quickly, and whether these concentrations can be maintained within (i.e. without exceeding) the effective range for a sufficient period of time. CsA itself seems kinetically adequate in this respect. In experimental animals, CsA reduces infarct size when introduced at the time of reperfusion [11]. In patients treated for acute myocardial infarction, CsA yields some protection against RI when administered intravenously immediately before coronary angioplasty [33]. Equally encouraging, conjugation to TPP$^+$ has been used to deliver a wide range of lipophilic compounds to mitochondria in tissues and does so quickly, achieving maximal levels in the heart within 4 min of intravenous injection and maintaining these for >1 h [34].

REFERENCES

1 Crompton, M. and Costi, A (1988) Kinetic evidence for a heart mitochondrial pore activated by Ca^{2+}, inorganic phosphate, and oxidative stress. A potential mechanism for mitochondrial dysfunction during cellular Ca^{2+} overload. Eur. J. Biochem. **178**, 489–581

2 Duchen, M. R., McGuinness, O., Brown, L. A. and Crompton, M. (1993) On the involvement of a cyclosporin A sensitive mitochondrial pore in myocardial reperfusion injury. Cardiovasc. Res. **27**, 1790–1794

3 Haworth, R. A. and Hunter, P. R. (1979) The Ca^{2+} induced membrane transition in mitochondria. III. Transitional Ca^{2+} release. Arch. Biochem. Biophys. **195**, 468–477

4 Crompton, M., Virji, S. and Ward, J. M. (1998) Cyclophilin-D binds strongly to complexes of the voltage dependent anion channel and the adenine nucleotide translocase to form the permeability transition pore. Eur. J. Biochem. **258**, 729–753

5 Crompton, M., Barksby, E., Johnson, N. and Capano, M. (2002) Mitochondrial intermembrane junctional complexes and their involvement in cell death. Biochimie **84**, 143–152

6 Brustovetsky, N., Tropschug, M., Heimpel, S., Heidkaemper, D. and Klingenberg, M. (2002) A large Ca^{2+} dependent channel formed by recombinant ADP/ATP carrier from *Neurospora crassa* resembles the mitochondrial permeability transition pore. Biochemistry **41**, 11804–11811

7 Leung, A.W.C., Varayuwatana, P. and Halestrap, A. P. (2008) The mitochondrial phosphate carrier interacts with cyclophilin D and may play a role in the permeability transition. J. Biol. Chem. **283**, 26312–26323

8 Shulga, N. and Pastorino, J. G. (2010) Ethanol sensitises mitochondria to the permeability transition by inhibiting deacetylation of cyclophilin-D mediated by sirtuin-3. J. Cell Sci. **123**, 4117–4127

9 Nazareth, W., Yafei, N. and Crompton, M. (1991) Inhibition of anoxia-induced injury in heart myocytes by cyclosporin A. J. Mol. Cell. Cardiol. **23**, 1351–1354

10 Griffiths, E. J. and Halestrap, A. P. (1993) Protection by cyclosporin A of ischaemia-reperfusion induced damage in isolated rat hearts. J. Mol. Cell Cardiol. **25**, 1461–1469

11 Lim, S. Y., Davidson, S. M., Hausenloy, D. J. and Yellon, D. M. (2007) Preconditioning and postconditioning: the essential role of the mitochondrial permeability transition pore. Cardiovasc. Res. **75**, 530–535

12 Li, Y., Johnson, N., Capano, M., Edwards, M. and Crompton, M. (2004) Cyclophilin-D promotes the mitochondrial permeability transition but has opposite effects on apoptosis and necrosis. Biochem. J. **383**, 101–109

13 Basso, E., Fante, L., Fowlkes, J., Petronilli, V., Forte, M. A. and Bernardi, P. (2005) Properties of the mitochondrial permeability transition pore in mitochondria devoid of cyclophilin D. J. Biol. Chem. **280**, 18558–18561

14 Baines, C. P., Kaiser, R. A., Purcell, N. H., Blair, N. S., Osinska, H., Hambleton, M. A., Brunskill, E. W., Sayen, R. M., Gottlieb, R. A., Dorn, G. W. et al. (2005) Loss of cyclophilin D reveals a critical role for the permeability transition in cell death. Nature **434**, 658–662

15 Schinzel, A. C., Takeuchi, O., Huang, Z., Fisher, J. K., Zhou, Z., Rubens, J., Hetz, C., Danial, N. N., Moskowitz, M. A. and Korsmeyer, S. J. (2005) Cyclophilin D is a component of the mitochondrial permeability transition and mediates neuronal cell death after focal cerebral ischaemia. Proc. Natl. Acad. Sci. U.S.A. **102**, 12005–12010

16 Devalararja-Narashimha, K., Diener, A. M. and Padanilam, B. B. (2009) Cyclophilin D gene ablation protects mice from ischaemic renal injury. Am. J. Physiol. Renal Physiol. **297**, F749–F759

17 Du, H., Guo, L., Fang, F., Chen, D., Sosunov, A. A., McKhann, G. M., Yan, Y. L., Wang, C. Y., Zhang, H., Molkentin, J. D. et al. (2008) Cyclophilin-D deficiency attenuates mitochondrial and neuronal perturbation and ameliorates learning and memory in Alzheimers disease. Nat. Med. **14**, 1097–1105

18 Forte, F., Gold, B. G., Marracci, G., Chaudhary, P., Basso, E., Johnsen, D., Yu, X., Fowlkes, J., Rahder, M., Stem, K., Bernadi, P. and Bourdette, D. (2007) Cyclophilin D inactivation protects axons in experimental autoimmune encephalomyelitis, an animal model of multiple sclerosis. Proc. Natl. Acad. Sci. U.S.A. **104**, 7558–7563

19 Millay, D. P., Sargent, M. A., Osinska, H., Baines, C. P., Barton, E. R., Vuagniaux, G., Sweeney, H. L., Robbins, J. and Molkentin, J. D. (2008) Genetic and pharmacologic inhibition of mitochondrial-dependent necrosis attenuates muscular dystrophy. Nat. Med. **14**, 442–447

20 Martin, L. J. (2010) The mitochondrial permeability transition pore: a molecular target for amyotrophic lateral sclerosis therapy. Biochim. Biophys. Acta **1802**, 186–197

21 Malouitre, S., Dube, H., Selwood, D. and Crompton, M. (2010) Mitochondrial targeting of cyclosporin A enables selective inhibition of cyclophilin-D and enhanced cytoprotection after glucose and oxygen deprivation. Biochem. J. **425**, 137–148

22 Haugland, R. P., Malekzadeh, M. N. and Zhang, Y. (1995) Diaminoxanthines. U.K. Pat. GB2283744A

23 Doyle, V., Virji, S. and Crompton, M. (1999) Evidence that cyclophilin A protects cells against oxidative stress. Biochem. J. **341**, 127–132

24 Taylor, P. T., Husi, H., Kontopidis, G. and Walkinshaw, M. D. (1997) Structures of cyclophilin-ligand complexes. Prog. Biophys. Mol. Biol. **67**, 155–181

25 Kajitana, K., Fujihashi, M., Kobayashi, Y., Shimizu, S., Tsujimoto, Y. and Miki, Y. (2008) The crystal structure of human cyclophilin-D at 0.96 angstrom resolution. Proteins **70**, 1635–1639

26 Jin, L. and Harrison, S. C. (2002) Crystal structure of human calcineurin complexed with cyclosporine A and human calcineurin. Proc. Natl. Acad. Sci. U.S.A. **99**, 13522–13526

27 McGuinness, O. M., Yafei, N., Costi, A. and Crompton, M. (1990) The presence of two classes of high affinity cyclosporin A binding sites in mitochondria. Evidence that the minor component is involved in the opening of an inner-membrane, Ca^{2+}-dependent pore. Eur. J. Biochem. **194**, 671–679

28 James, A. M., Sharpley, M. S., Manus, A.R.B., Frerman, F. E., Hirst, J., Smith, R.A.J. and Murphy, M. P. (2007) Interaction of the mitochondrial-targeted antioxidant mitoQ with phospholipid bilayers and ubiquinone oxidoreductase. J. Biol. Chem. **282**, 14708–14718

29 Venardos, K. M. and Kaye, D. M. (2007) Myocardial ischaemia-reperfusion injury, antioxidant systems and selenium. A review. Curr. Med. Chem. **14**, 1539–1549

30 Kim, J. S., Jin, Y. G. and Lemasters, J. J. (2006) Reactive oxygen species, but not Ca^{2+} overloading, trigger pH- and mitochondrial permeability transition-dependent death of adult rat myocytes after ischaemia-reperfusion. Am. J. Physiol. Heart Circ. Physiol. **290**, H2024–H2034

31 Kim, J., Choi, T. G. and Ding, Y. (2008) Overexpressed cyclophilin-B suppresses apoptosis associated with ROS and Ca^{2+} homeostasis after endoplasmic reticulum stress. J. Cell Sci. **121**, 3636–3648

32 Griffiths, E. J., Ocampo, C. J., Savage, J. S., Rutter, G. A., Hansford, R. G., Stern, M. D. and Silverman, H. S. (1998) Mitochondrial calcium transporting pathways during hypoxia and reoxygenation in single cardiomyocytes. Cardiovasc. Res. **39**, 423–433

33 Piot, C., Croisille, P., Staat, P., Thibault, M. D., Rioufol, G., Mewton, M., Elbelghiti, R., Cung, T. T., Bonnefoy, E., Angoulvant, D. et al. (2008) Effect of cyclosporine on reperfusion injury in acute myocardial infarction. N. Engl. J. Med. **359**, 473–481

34 Porteous, C. M., Logan, A., Evans, C., Ledgerwood, E. C., Menon, D. K., Aigbirhio, F., Smith, R.A.J. and Murphy, M. P. (2010) Rapid uptake of lipophilic triphosphonium cations by mitochondria *in vivo*: Implications for mitochondria-specific therapies and probes. Biochim. Biophys. Acta **1800**, 1009–1017